Analytical Methods

PAPER

Cite this: *Anal. Methods*, 2019, **11**, 1551

Influence of TiO_2 and ZrO_2 nanoparticles deposition on a stainless steel furnace used for trace element determination by TS-FF-AAS†

G. Carrone,[a]* D. Onna,[b]* E. Morzan,[c] R. Candal,[a] Y. S. Minaberry,[d] J. Schneider[d] and M. Tudino[d]

Received 9th January 2019
Accepted 13th February 2019

DOI: 10.1039/c9ay00063a

rsc.li/methods

In this study, we presented the influence of nanoparticle coatings over the inner furnace wall used in TS-FF-AAS for the determination of trace elements (Ag, Cd, Pb, and Se) in different complex matrix. The use of ceramic nanomaterials (ZrO_2 and TiO_2) as a coating, produced by the dipcoating technique, enabled enhanced analytical performance (analytical response, sensitivity, LOD, LOQ, and signal stability). This furnace modification was used for determining the analytes in different samples.

Introduction

Atomic Absorption Spectrometry (AAS) is a widely used technique for the determination of trace elements in different kinds of samples. Flame Atomic Absorption Spectrometry (FAAS) was introduced by Walsh in 1955;[1] since then, several modifications of this technique have been made in order to increase its analytical performance. A significant improvement done by Gáspár and Berndt[2] involved placing an atomization tube onto the combustion flame, complete sample introduction and confining it in a reduced volume. This improvement extended the residence time of the atomic vapor within the light source pathway. This method, called Thermospray Flame Furnace Atomic Absorption Spectrometry (TS-FF-AAS),[3] exhibited a significant sensitivity. Since then, several works have been published using TS-FF-AAS for the determination of several trace elements, particularly the more volatile ones.[4]

A standard setup for this technique involved injecting a liquid sample into a Ni furnace through a ceramic capillary heated by an air/acetylene flame. The original setup had been changed in order to improve the analytical performance, which was done by changing either the heating source[5,6] or the furnace material. The majority of the literature used nickel-based alloys with regard to furnace material. However, Ti or quartz had been employed as furnaces, which showed an improvement in the analytical performance.[7] Nevertheless, these materials were more expensive than the traditional nickel furnaces. In search for more economic alternatives, stainless steel was employed in EMFAAS (Electrothermal Metallic Furnace Atomic Absorption Spectrometry).[6,8] Even though stainless steel is one of the less expensive alloys that are resistant to high temperatures, it is not the best choice for TS-FF-AAS mainly due to its low thermal stability that leads to an impoverishment of the analytical figures of merit.

Coatings of ceramic materials over stainless steel[9] could be a convenient way to obtain an improvement in the sample atomization process.[10] In addition, some studies have also showed an enhancement in the analytical performance due to the interaction between some particular analytes and the ceramic material, *e.g.* TiO_2.[11] From this perspective, we employed stainless steel coated with TiO_2 or ZrO_2 nanoparticles (NPs) as a flame furnace.

In this study, we presented the determination of trace elements (Ag, Cd, Pb, and Se) using the TS-FF-AAS method. In particular, the coated tubes exhibited an improvement in the analytical performance, compared with a bare stainless steel tube. The analytical signal stability and reproducibility from the coated tubes are quite remarkable. These furnaces were used to determine trace elements such as Ag, Cd, Pb, and Se in different samples.

Experimental

All solutions were prepared with analytical grade chemical reagents and double-deionized water (DDW) was obtained from a Milli-Q purification system (Millipore, Bedford, MA, USA). All glasswares were washed with EXTRAN (Merck) 1% v/v and kept

[a]*Instituto de Investigación e Ingeniería Ambiental (IIIA), Universidad Nacional de San Martin, CONICET, 3iA, Campus Miguelete, 25 de Mayo y Francia, 1650, San Martin, Provincia de Buenos Aires, Argentina. E-mail: carroneguillermo@gmail.com*

[b]*Instituto de Nanosistemas, CONICET, Universidad Nacional de San Martin, Campus Miguelete, 25 de Mayo y Francia, 1650, San Martin, Buenos Aires, Argentina. E-mail: diego.onna@qi.fcen.uba.ar*

[c]*Comisión Nacional de Energía Atómica, General Paz 1499, Buenos Aires, B1950KNA, Argentina*

[d]*Laboratorio de Trazas, DQIAQF, Facultad de Ciencias Exactas y Naturales, Universidad de Buenos Aires, Ciudad Universitaria Pab. II, C1428EHA, Buenos Aires, Argentina*

† Electronic supplementary information (ESI) available. See DOI: 10.1039/c9ay00063a

in 10% v/v HCl with further cleaning using DDW. Standard solutions of the studied analytes were prepared by the appropriate dilution of 1.000 g L^{-1} stock solution (Merck Darmstadt, Germany). Commercially available reagents (Sigma Aldrich) were used as received for the nanoparticle synthesis.

Instrument

An atomic absorption spectrometer Shimadzu AA6800 (Shimadzu, Kyoto, Japan), hollow cathode lamps (Hamamatsu, Japan) and a deuterium lamp for background correction were employed throughout the measurements. Other instrumental conditions were those provided by the manufacturer. The TS-FF-AAS system was assembled with a peristaltic pump with eight channels and six rollers (IPC, Ismatec, Glattbrugg-Zurich, Switzerland), and a six-port rotary valve VICI (Valco Instruments, Houston, TX, USA). About 500 μL of the sample solution was introduced into a carrier stream (DIW) and then injected into the furnace through a ceramic capillary (0.5 mm i.d., 6 cm length). The furnace (316 L stainless steel tube, 10 cm length, 1 cm i.d., with six holes) was mounted on an air/acetylene flame with the assistance of a homemade holder. The furnace was placed in the optical path of the spectrometer and employed as an absorption cell throughout the experiments.

Stainless steel flame furnace atomizer preparation

The stainless steel tubes were thoroughly washed in acetone to remove grease and other debris. Then, they were treated with a 10% w/w phosphoric acid solution in an ultrasonic bath (Testlab TB-024 TD CD), rinsed with water and annealed in air at 500 °C for 1 h.

Nanoparticle synthesis and deposition

The syntheses of the sols were based on previously reported procedures.[9] For titania coatings, titanium isopropoxide ($Ti(OC_3H_7)_4$) was used as a precursor, isopropanol (C_3H_7OH) was used as a solvent and glacial acetic acid (CH_3COOH) was used as a catalyst. The titania sol was prepared by dissolving $Ti(OC_3H_7)_4$ in isopropanol and then, acetic acid was added. The volume ratios of $C_3H_7OH/Ti(OC_3H_7)_4$ and $CH_3COOH/Ti(OC_3H_7)_4$ were 7 and 2, respectively. For zirconia coatings, zirconium isopropoxide ($Zr(OC_3H_7)_4$) was used as a source of zirconia. The sol was prepared by dissolving the alkoxide in isopropanol (C_3H_7OH). Consequently, acetic acid (CH_3OOH) and water were added. The volume ratios of $H_2O/Zr(OC_3H_7)_4$, H_2O/C_3H_7OH, and H_2O/CH_3COOH were 4, 1.33, and 2, respectively. The mixtures were immersed in an ultrasonic bath (Testlab TB-024 TD CD). After 30 min, the resulting sol was homogenized and maintained at −4 °C.

A coated sample was prepared by a dip coating technique. First, the sample was annealed at 500 °C in air for 1 hour in order to improve its affinity for the oxide sols and reduce its contact angle. Then, the substrate was withdrawn from the sol at a constant rate of 10 cm min^{-1}. The resulting sample was dried at 120 °C for 15 minutes and then 5 more coatings were applied. The 6 times coated sample was thermally treated at 800 °C for 1 hour with a 5 °C min^{-1} ramp.

Coating characterization

The morphology of the coatings was studied using a scanning electron microscopic (SEM) technique utilizing an SUPRATM 40 field emission SEM (Carl Zeiss SMT AG) working at an electron beam energy of 3 keV. The chemical composition was determined by a semi-quantitative energy dispersive X-ray spectroscopic (EDS) technique utilizing an Oxford Instruments INCA system. The coatings were deposited over the stainless steel 316 L plate straps for SEM and EDS characterizations.

Temperature measurement

Temperature measurements of the furnace were done by an imaging method using a RGB digital camera (Samsung NX-1100). The green channel (G) was used for processing images; therefore, the emitted light intensity fits in the dynamic range of the camera detector. Images were processed with a public software ImageJ®[12] using the method described in the literature.[6]

Results and discussion

Deposition of NPs on furnace surface

The application of ceramic coatings on the surface of the stainless steel furnace is a common method to extend the resistance of steel towards corrosion. The coating serves as a way to passivate the surface.[9] In general, these thin films needed good adherence and compatible mechanical properties to the substrate. Thin films made using NP sols fulfil these requirements, and so they are a common strategy to modify the steel surfaces.[9] A challenge of these systems was achieving a homogeneous coating on non-flat surfaces. A practical application method for substrates that do not possess a planar geometry was dip coating.

In this study, TiO_2 and ZrO_2 NPs were used to coat the stainless steel 316 L tube. As a result of the annealing treatment being done prior to the dip coating process, the steel surface changed to a black color, which evidenced the formation of iron oxide. Fig. 1 shows the SEM images of the surface of stainless steel after thermal treatment and after applying different coatings. As shown in Fig. 1A, the surface exhibited iron oxide crystals with smooth surfaces and sizes larger than 200 nm. In addition, images of those coated with TiO_2 and ZrO_2 are shown in Fig. 1B and C, respectively. The presence of titania and zirconia in these coatings was confirmed by an energy dispersive X-ray spectroscopy (EDS), as shown in ESI.† Compared with the bare surface, both the coatings presented NPs with an average size of 20 nm. The coatings were homogeneous and covered the entire steel surface, which showed a good adherence of the nanoparticles over the iron oxide during the sample manipulation.

After the exposure to the air/acetylene flame, the bare surface showed an increment in the size of iron oxide crystals (Fig. 1D). Similarly, the nanoparticles on the coated steel underwent a sinterization process due to the high temperatures. Sintering occurred when packed nanoparticles were heated to a temperature where their atoms diffuse and bonds between nanoparticles were formed.[13] This process led to an increase in the

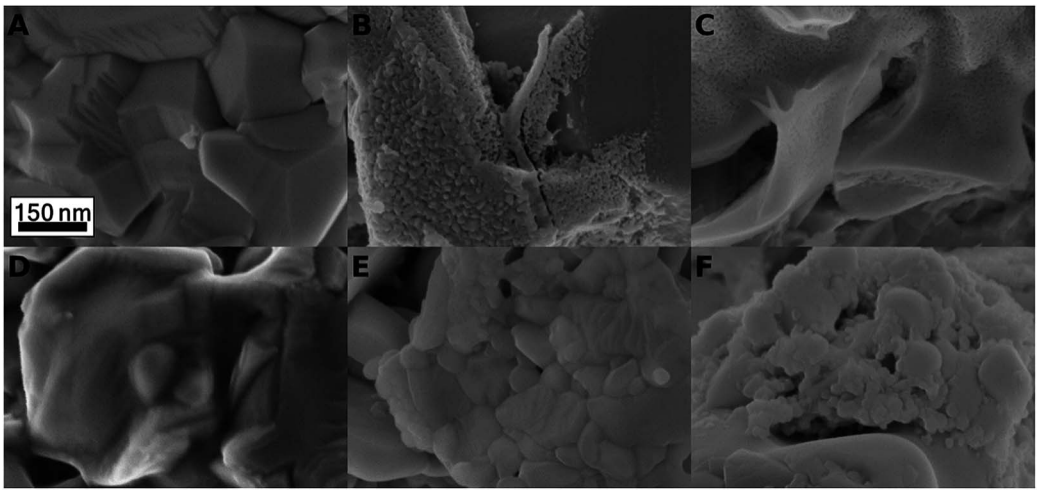

Fig. 1 SEM images of (A) uncoated 316 L steel oxidized at 500 °C for 1 h before acetylene flame (BAF), (B) TiO_2 coated 316 L steel annealed at 500 °C for 1 h, coated 6 times and annealed at 800 °C for 1 h BAF, (C) ZrO_2 coated 316 L steel oxidized at 500 °C for 1 h, coated 6 times and annealed at 800 °C for 1 h BAF, (D) sample A after acetylene flame (AAF), (E) sample B AAF, and (F) sample C AAF.

nanoparticle sizes. Indeed, it is observed in Fig. 1E and F in comparison to the samples without exposure to the air/acetylene flame. The results after the air/acetylene flame exposure indicated that within the flame, the nanoparticles were stable and the coating was robust enough to modify the iron oxide surface at high was a desirable property for enhancing the analytical performance of the TS-FF-AAS method, essentially the lifetime of the modified furnace.

Analytical sensitivity of different furnaces

The analytical responses for solutions containing Cd, Pb, Ag, and Se obtained with the different furnace coatings are shown in Fig. 2. In general, the analytical signal and the sensitivity improved when the stainless steel furnaces were coated with NPs in comparison to the bare furnaces. In addition, the LOD (3 s) and experimental LOQ decreased, while a shorter linear range (LR) was observed. Table 1 summarizes the figures of merit from the analytes' determination comparing the stainless steel furnace coated with TiO_2 (TiO_2@steel), ZrO_2 (ZrO_2@steel), or uncoated.

The increment in the sensitivity of TiO_2@steel furnaces with respect to the bare ones was 13%, 64%, 15%, and 91% for Ag, Cd, Pb, and Se, respectively. In the case of ZrO_2@steel furnaces, the increment in sensitivity was 102%, 113%, and 19% for Ag, Cd, and Se, respectively. However, in the case of Pb no increase was observed. The increase in the analytical signal may be explained by two hypotheses; however, a deeper study must be conducted in order to determine the origin of the phenomenon. First, an increase in the thermal homogeneity inside the tubes, which was provided by the use of ceramic materials, and second, for some cases, the contribution of coating–analyte interaction that favored atomization; therefore, enhancing the signal (*vide infra*).

The calculated limits of detection (LOD, 3 s) showed changes due to the presence of coating (Table 1). For Cd and Pb, the LOD decreased by one order of magnitude as a consequence of the coating. While for Ag and Se, the LOD had almost the same value regardless of the coating. In addition, for all the cases, the experimental limit of quantification (LOQ) of the coated furnaces improved for all the analytes, as the linear range began at the lower concentration values. This improvement implied that modification of the inner furnace wall allowed the quantification of lower concentrations. In addition, coated furnaces showed a similar analytical performance as the conventional Ni furnace. Results are summarized in a table shown in ESI.†

The relative standard deviations (RSD%, $n = 3$) for the analytes under study using the different furnaces are shown in Table 2. Results showed that the RSD% for the coated furnaces were smaller than the RSD% for the bare steel furnace. In addition, the TiO_2 coated stainless steel tube displayed the highest reproducibility.

Effect of the flow rate on the furnace temperature and the analytical responses of Ag, Cd, Pb and Se employing different surfaces

The analytical response at 100 μg Cd per L level for flow rates ranging between 0.6 and 2.1 mL min^{-1} is shown in Fig. 3. As the sample entered into the furnace, a decrease in the temperature was expected. Thus, the increase in the flow rate would yield a more significant temperature decrement and a lowered analytical response. The same behaviour was observed for the bare steel furnace, as observed in similar systems used elsewhere.[6,8,14] In the case of coated furnaces, the analytical response remained almost constant while the injection flow rate was increased. The same procedure was done for Ag, Pb and Se at 500, 300 and 1000 μg L^{-1} levels, respectively, and the results are shown in ESI.† For these cases, coated furnaces generally present a higher signal reproducibility while the flow rate was increased. But the signal decreased onwards a flow rate value for all furnaces (coated and uncoated). This decrement in general followed the order: ZrO_2@steel < TiO_2@steel < bare steel. A possible explanation for this behaviour could be

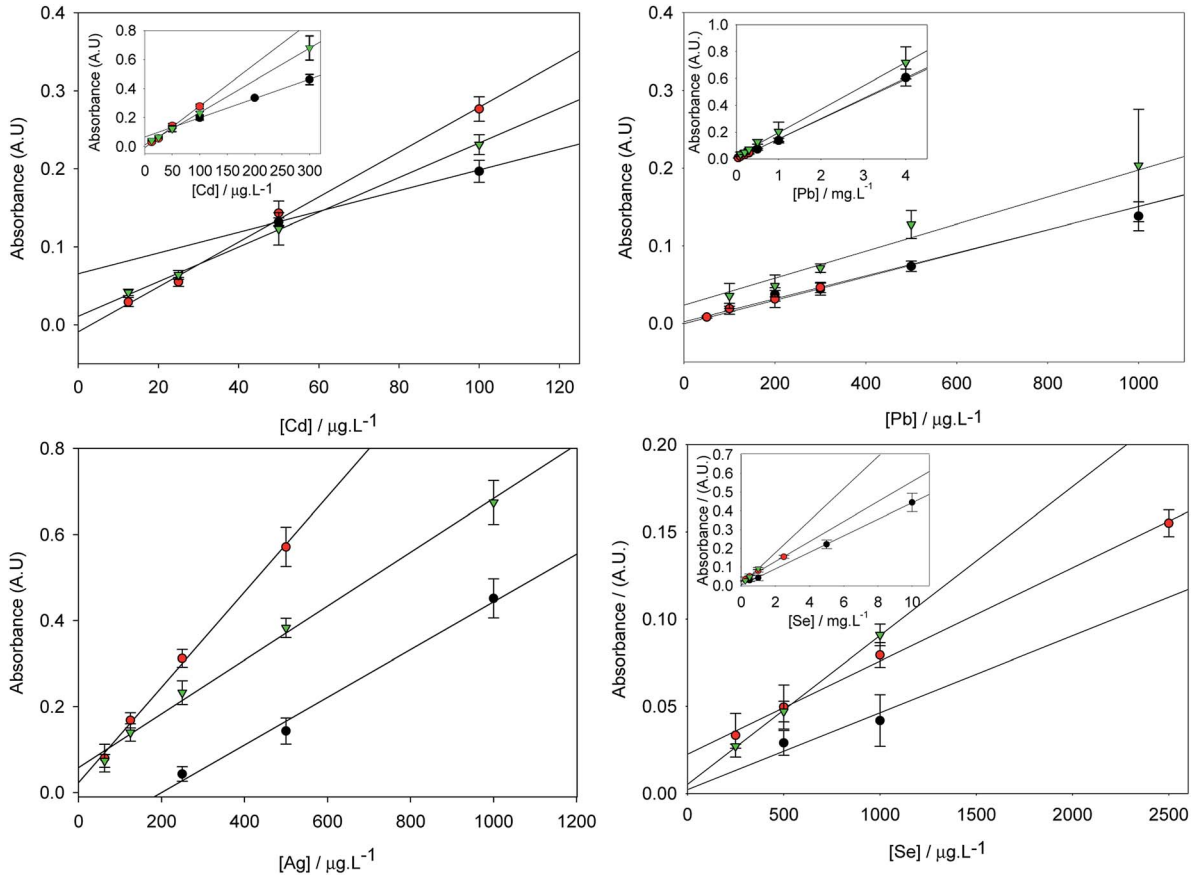

Fig. 2 Analytical responses of solutions containing Cd, Pb, Ag and Se, which were obtained using furnace of bare steel (black), ZrO_2@steel (red) and TiO_2@steel (green). Flow rate is 0.8 mL min^{-1}.

attributed to a higher temperature or thermal homogeneity inside the furnace. Thus, analysing the furnace temperature was needed to rationalize the coating effect.

In order to determine the temperatures (and their spatial distributions) for the different furnaces, the temperature of the internal surface when varying the injection flow rate was approximated by the external temperature. This can be measured by using an already developed imaging method.[5] Results of this method are shown in ESI.† Two behaviours were observed: (i) the bare steel furnace exhibited a higher temperature than the coated one and (ii) the thermal homogeneity in the volatilization area was greater for coated furnaces than for bare steel furnaces. From these results, it was possible to infer that the thermal homogeneity was related to a better vaporization (see ESI†) and this yielded a better atomization process, which increased the analytical signal. In addition, the TiO_2@steel furnace showed a higher analytical response for some analytes (Pb and Se) (Fig. 2). These behaviours suggested that the NP coating due to its chemical composition might act as a catalyst, enhancing the analytical signal. The interaction between the analyte and the coating lowered the atomization temperature, which increased the analytical signal as described for copper determination.[11]

In order to quantify this process, another study should be conducted separately for each case and with an AAS method that allowed a better thermal control and homogeneity, for example EMFAAS.[5]

The particular case of Cu was studied using the TiO_2@steel furnace and bare steel furnace; results showed an improvement in the analytical response and sensitivity when using TiO_2@steel furnace compared to bare steel furnace (see ESI†). This confirmed the hypothesis that there was a catalytic interaction between the analyte (Cu) and the furnace material (TiO_2) that favoured the atomization process. Nevertheless, as Cu was one of the components of stainless steel 316 L, although the percentage of it was low (about 1%), variations in the furnace temperature generated changes in the analytical signal, detecting a lower reproducibility and stability of the signal. Then for the other analytes present in the steel (Fe, Ni, Cr, Mn, Cu, *etc.*), it was advisable to use another material as a support for the deposition of the nanoparticles.

Analytical response in the presence of interferents

Fig. 4 presents the relative analytical responses obtained for Cd and Pb in the presence of different anions. For the bare steel furnaces, the signal of Cd (at 100 µg L^{-1} level) presented an enhancement of the analytical signal. In contrast, the coated furnaces did not exhibit these changes. The behavior of the bare steel tube can be attributed to a catalytical process during the

Table 1 Figures of merit for the determination of Ag, Cd, Pb and Se employing bare and modified stainless steel furnaces[a]

Analyte	Ag			Cd			Pb			Se		
Furnace	Bare steel	TiO_2@steel	ZrO_2@steel	Bare steel	TiO_2@steel	ZrO_2@steel	Bare steel	TiO_2@steel	ZrO_2@steel	Bare steel	TiO_2@steel	ZrO_2@steel
Dynamic range (μg L^{-1})	250–1000	63–500	63–500	50–300	12.5–300	12.5–100	200–4000	50–300	100–4000	500–10 000	250–1000	250–2500
Limit of detection (μg L^{-1})	9	7	7	5	0.5	0.4	22	4	7	96	71	92
Sensitivity (L μg^{-1})	5.54×10^{-4}	6.26×10^{-4}	1.12×10^{-3}	1.35×10^{-3}	2.22×10^{-3}	2.88×10^{-3}	1.53×10^{-4}	1.76×10^{-4}	1.48×10^{-4}	4.47×10^{-5}	8.54×10^{-5}	5.34×10^{-5}
Sensitivity increase[b]	—	13%	102%	—	64%	113%	—	15%	−7%	—	91%	19%

[a] TiO_2@steel: furnace coated with TiO_2 and ZrO_2@steel: furnace coated with ZrO_2. [b] Compared to bare steel furnace.

Table 2 Relative standard deviation% (RSD%) at 0.8 mL min^{-1} injection flow rate ($n = 3$)

Furnace	Cd at 100 μg L^{-1} level	Pb at 300 μg L^{-1} level	Se at 1000 μg L^{-1} level	Ag at 500 μg L^{-1} level
Bare steel	7.18	17.6	35.5	21.2
TiO_2@steel	5.52	7.52	6.79	5.88
ZrO_2@steel	5.71	14.3	8.95	8.03

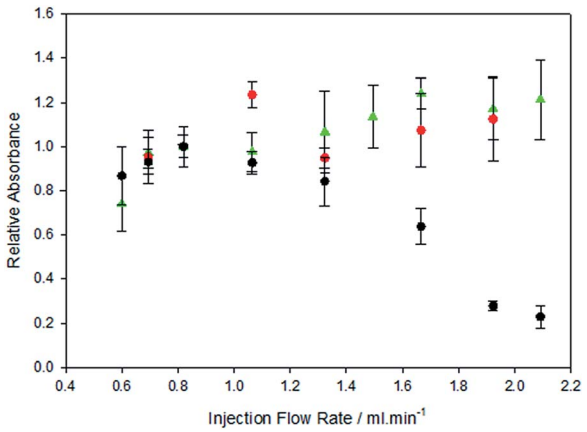

Fig. 3 Analytical response of Cd, at 100 μg L^{-1} level, at different injection flow rates, using furnace of bare steel (black), ZrO_2@steel (red) and TiO_2@steel (green). It is noteworthy that the absorbances were divided by the absorbances at 0.8 mL min^{-1} flow rate.

atomization of the analyte, which was influenced by the interferent ion at the moment of interacting with the furnace surface (iron oxide). In the case of Pb (at 300 μg L^{-1} level), a lower analytical signal for the bare steel furnace was observed, which was not the case for the employment of the coated furnaces.

Furnace lifetime and reusability

The main cause that shortened the lifetime of the coated furnace was the formation of iron oxide during the cooling: an iron oxide layer growth and a detachment of the coating occurred. In the case studied, solutions containing 12.5–300 μg L^{-1} of Cd were measured during a period of 200 shots (30 per hour) using a coated furnace. Throughout these measurements, the analytical response remained stable.

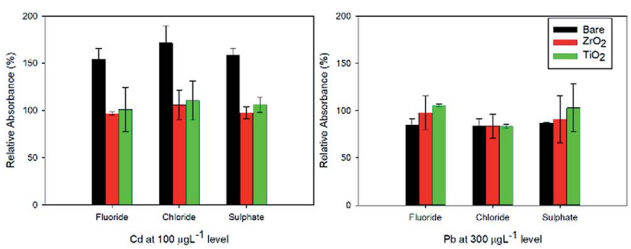

Fig. 4 Analytical signals obtained for 100 μg Cd per L (left) and 300 μg Pb per L (right) in water in the presence of different anions (sodium salt) at 1000 μg L^{-1}.

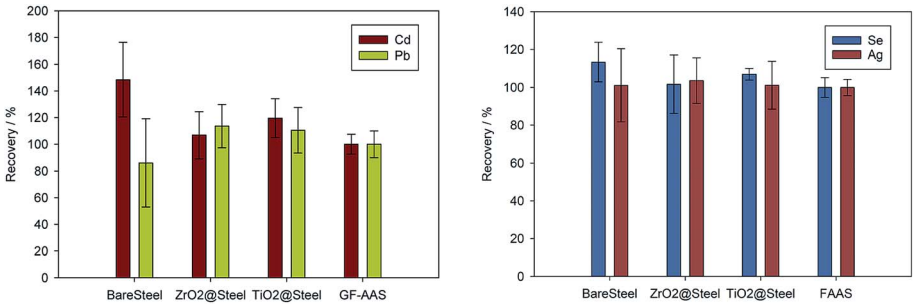

Fig. 5 Percentage of recovery for the determination of Cd and Pb in river water, Se in dietary supplement and Ag in topical cream using the different furnaces and the referee methodology.

This could be produced by the reductive flame of acetylene/air, which prevented the growth of the iron oxide layer and kept the NPs attached to the stainless steel surface. However, after turning off the flame and cooling the furnace, the difference between the coefficients of thermal expansion of the stainless steel and the coating produced a detachment of the NPs. These led to a loss of the properties of the coated furnace (ESI†), which started behaving as the bare ones.

In order to evaluate if the samples containing high amounts of Fe decreased the furnace lifetime or analytical performance of the technique, determination of Cd at 100 μg L^{-1} level was done, before and after injecting solutions containing 1 g L^{-1} of Fe and a saturated solution of $FeSO_4$ during 60 and 30 minutes, respectively, into the furnace. No changes were observed, showing that high content of Fe did not affect the analytical performance of the method and furnace lifetime.

Even though abrupt changes in the temperature during the cooling decreased the coating lifetime, the coating reusability could be carried out simply and economically. The coating reusability involved cleaning the furnace with 10% w/w H_3PO_4 in an ultrasonic bath, heating 1 h at 500 °C and then applying the 6 layers of coating. The resulting coated furnace presented a highly reproducible and constant analytical signal after several times of reusing the same furnace (ESI†).

Determination of Cd and Pb in river sample

Different furnaces were employed for Cd and Pb determination in a river sample (collected from Reconquista River, Buenos Aires province, Argentina). Samples were analysed by the standard-addition method. Results were compared to the ones obtained using GF-AAS as referee methodology for Cd and Pb determination (64.7 ± 4.8 μg L^{-1} and 41.5 ± 4.1 μg L^{-1}, respectively, for Cd and Pb).

Fig. 5, left, shows the recovery percentage obtained for the determination of Cd and Pb in river sample using the different furnaces. In this case, the coated furnaces showed an almost 100% recovery. Although for bare steel furnace a positively biased error was observed for Cd determination, Pb showed a negative one. In addition, the standard deviation was considerably higher for bare steel furnace. These results confirmed that the coated furnaces improved the determination of trace elements compared to the bare steel ones.

Also, samples containing Ag (topical antibiotic cream, 1% silver sulfadiazine) and Se (dietary supplement, 200 μg per tablet), were digested in a solution prepared with 20 mL of HNO_3 (65%) and 10 mL of H_2O_2 (8% v/v) for 1 h at the boiling point and analysed. Results were compared using FAAS as a referee methodology (Fig. 5, right). For the case of Ag (FAAS determination, 1.008 g per 100 g of topical cream), coated furnaces showed a higher reproducibility than the bare steel furnace. Nevertheless, all the furnaces presented a percentage of recovery nearly 100%. In the case of Se (FAAS determination, 327.9 μg per tablet), the coated furnaces showed a better percentage of recovery.

Conclusions

We have designed different coatings (NPs TiO_2 and ZrO_2) for the inner wall of the furnace used in the TS-FF-AAS method, obtaining an improvement in the analytical performance of the AAS technique for the determination of several analytes (Ag, Cd, Pb and Se). Higher responses were obtained, sensitivities were increased up to 100% and a decrease in LOQ and LOD was observed for all the cases (highlighting the case of Cd > 1000%).

Temperature measurements have been recorded using an imaging method in order to analyse the homogeneity of this variable and its influence on the atomization process. An increment in the thermic homogeneity and stability was observed for the coated furnaces in comparison with the bare steel ones. Although the response of the analytes towards the different coated furnaces did not show a definite correlation with the increase in the analytical signal, two hypotheses can be taken into account: (i) the improvement in the atomization of the sample due to a greater thermal stability and homogeneity obtained by ceramic materials coatings and (ii) the interaction of the analyte with the metal surface that could catalyse the atomization process.

The method was successfully applied for the determination of the studied analytes in different matrix, and the analytical results were compared with a referee methodology.

Conflicts of interest

There are no conflicts of interest to declare.

Acknowledgements

This research was supported by the National University of San Martin, the National Agency for Science and Technology Promotion (CONICET), and the University of Buenos Aires. GC is a research fellow of UNSAM (Universidad Nacional de San Martin); DO, YM, RC and MT are members of CONICET; EM is a member of CNEA (Comisión Nacional de Energía Atómica) and JS is a research fellow of UBA (Universidad de Buenos Aires). We thank Cecilia Canteras for the river water samples and Claudia Marchi for SEM micrographs.

Notes and references

1 A. Walsh, *Spectrochim. Acta*, 1955, **7**, 108.
2 A. Gáspár and H. Berndt, *Anal. Chem.*, 2000, **72**, 240.
3 (*a*) A. Gáspár and H. Berndt, *Spectrochim. Acta, Part B*, 2000, **55**, 587; (*b*) M. L. Brancalion, E. Sabadini and M. A. Z. Arruda, *Anal. Chem.*, 2007, **79**, 6527; (*c*) M. A. Z. Arruda and E. C. Figueredo, *Spectrochim. Acta, Part B*, 2009, **64**, 477; (*d*) K. Miranda and E. R. Pereira-Filho, *Anal. Methods*, 2009, **1**, 215.
4 (*a*) E. R. Pereira-Filho, H. Berndt and M. A. Z. Arruda, *J. Anal. At. Spectrom.*, 2002, **17**(10), 1308; (*b*) C. C. Nascentes, M. Y. Kamogawa, K. G. Fernandes, M. A. Z. Arruda, A. R. A. Nogueira and J. A. Nóbrega, *Spectrochim. Acta, Part B*, 2005, **60**(5), 749; (*c*) C. C. Nascentes, M. A. Z. Arruda, A. R. A. Nogueira and J. A. Nóbrega, *Talanta*, 2004, **64**, 912; (*d*) G. L. Donati, C. C. Nascentes, A. R. A. Nogueira, M. A. Z. Arruda and J. A. Nóbrega, *Microchem. J.*, 2006, **82**, 189.
5 (*a*) V. N. Muzgin, Y. B. Atnashev, V. E. Korepanov and A. A. Pupyshev, *Talanta*, 1987, **34**(1), 197; (*b*) J. A. Holcombe and D. L. Borges, Graphite Furnace Atomic Absorption Spectrometry, *Encyclopedia of Analytical Chemistry*, 2010.
6 E. Morzan, G. Carrone, M. Tudino and R. Etchenique, *Anal. Methods*, 2017, **9**, 756.
7 (*a*) M. A. Bezerra, V. A. Lemos, J. S. Garcia, D. G. da Silva, A. S. Araújo and M. A. Z. Arruda, *Talanta*, 2010, **82**(2), 437; (*b*) F. A. Lobo, A. C. Villafranca, A. P. de Oliveira and M. de Moraes, *At. Spectrosc.*, 2007, **28**, 17; (*c*) M. S. Gomes and E. R. Pereira-Filho, *Microchem. J.*, 2009, **93**, 93; (*d*) E. Morzan, O. Piano, J. Stripesky and M. Tudino, *Spectrochim. Acta, Part B*, 2012, **77**, 58.
8 G. Carrone, E. Morzan, M. Tudino and R. Etchenique, *J. Anal. At. Spectrom.*, 2018, **33**, 170.
9 (*a*) M. Atik and M. A. Aegerter, *J. Non-Cryst. Solids*, 1992, **147**, 183; (*b*) M. Atik, P. De Lima Neto, L. A. Avaca, M. A. Aegerter and J. Zarzycki, *J. Mater. Sci. Lett.*, 1994, **13**(15), 1081; (*c*) M. Atik, P. D. L. Neto, M. A. Aegerter and L. A. Avaca, *J. Appl. Electrochem.*, 1995, **25**(2), 142–148.
10 (*a*) J. D. Bernardin and I. Mudawar, *J. Heat Transfer*, 1999, **121**(4), 894; (*b*) H. Kim, B. Truong, J. Buongiorno and L. W. Hu, *J. Therm. Sci. Technol.*, 2012, **7**(3), 453; (*c*) G. Liang and I. Mudawar, *Int. J. Heat Mass Transfer*, 2017, **106**, 103; (*d*) S. H. Kim, Y. Jiang and H. Kim, *Exp. Therm. Fluid Sci.*, 2018, **99**, 85.
11 G. A. Petrucelli, P. K Stocco, M. I. M. S. Bueno and E. R. Pereira-Filho, *J. Anal. At. Spectrom.*, 2006, **21**(11), 1298.
12 C. A. Schneider, W. S. Rasband and K. W. Eliceiri, *Nat. Methods*, 2012, **9**(7), 671.
13 C. J. Brinker and G. W. Scherer, *Sol-gel science: the physics and chemistry of sol-gel processing*, Academic Press, 2013.
14 E. Morzan, J. Stripeikis, H. Goicoechea and M. Tudino, *Chemom. Intell. Lab. Syst.*, 2016, **151**, 44.